

Proteins mediating DNA loops effectively block transcription

Zsuzsanna Vörös, Yan Yan, Daniel T. Kovari, Laura Finzi ,* and David Dunlap*

Department of Physics, Emory University, Atlanta, Georgia 30322

Received 18 December 2016; Accepted 8 March 2017

DOI: 10.1002/pro.3156

Published online 14 March 2017 proteinscience.org

Abstract: Loops are ubiquitous topological elements formed when proteins simultaneously bind to two noncontiguous DNA sites. While a loop-mediating protein may regulate initiation at a promoter, the presence of the protein at the other site may be an obstacle for RNA polymerases (RNAP) transcribing a different gene. To test whether a DNA loop alters the extent to which a protein blocks transcription, the lac repressor (LacI) was used. The outcome of *in vitro* transcription along templates containing two LacI operators separated by 400 bp in the presence of LacI concentrations that produced both looped and unlooped molecules was visualized with scanning force microscopy (SFM). An analysis of transcription elongation complexes, moving for 60 s at an average of 10 nt/s on unlooped DNA templates, revealed that they more often surpassed LacI bound to the lower affinity O₂ operator than to the highest affinity O_s operator. However, this difference was abrogated in looped DNA molecules where LacI became a strong roadblock independently of the affinity of the operator. Recordings of transcription elongation complexes, using magnetic tweezers, confirmed that they halted for several minutes upon encountering a LacI bound to a single operator. The average pause lifetime is compatible with RNAP waiting for LacI dissociation, however, the LacI open conformation visualized in the SFM images also suggests that LacI could straddle RNAP to let it pass. Independently of the mechanism by which RNAP bypasses the LacI roadblock, the data indicate that an obstacle with looped topology more effectively interferes with transcription.

Keywords: transcription elongation; RNAP; lac repressor protein; DNA looping; scanning force microscopy; magnetic tweezers

Additional Supporting Information may be found in the online version of this article.

This is an open access article under the terms of the Creative Commons Attribution License, which permits use, distribution and reproduction in any medium, provided the original work is properly cited.

Statement: Protein-mediated DNA loops are a ubiquitous mechanism of transcriptional regulation. In such loops a protein bridges two distant sites, one of which is typically near the promoter to be regulated, while the other site may be in a different gene, and its occupation may be of hindrance to an elongating RNAP. Single molecule experiments reveal that a protein securing a loop is a stronger transcriptional roadblock than one bound to a single DNA site.

Grant sponsor: National Institutes of Health; Grant numbers: GM084070 and 3R01GM084070-07S1 to L.F.

*Correspondence: Laura Finzi, Department of Physics, Emory University, Atlanta, Georgia 30322. E-mail: lfinzi@emory.edu or David Dunlap, Department of Physics, Emory University, Atlanta, Georgia 30322. E-mail: ddunlap@emory.edu

Introduction

Proteins bound to DNA may act as roadblocks that hinder elongation by RNA polymerase during transcription. The mechanisms by which RNA polymerases might surpass such roadblocks are poorly understood. Previous single-molecule studies have focused on RNA polymerases disrupting nucleosomes.^{1–4} However, nucleosomes are only found in eukaryotes, interact with DNA nonspecifically, and are substrates for post-translational modifications that regulate chromatin remodeling and the recruitment of accessory factors that regulate transcription.⁵ In contrast, many transcription factors from organisms spanning all kingdoms recognize specific sites on DNA to shape the genome and regulate various genomic functions, and may or may not

undergo chemical modifications regulated by complex pathways. Very often they recognize multiple specific sequences to which they bind with different affinities and cooperatively.^{6,7} These tunable, cooperative interactions determine ubiquitous architectural DNA modifications such as DNA looping, the role of which has not been directly investigated in earlier studies on transcription roadblocks either *in vivo* or *in vitro*.

While a loop-mediating protein may regulate initiation from the promoter near one of the bridged binding sites, its presence at the other site may be an obstacle for RNA polymerases transcribing a different gene. To test whether a DNA loop alters the extent to which a protein halts transcription, the lac repressor protein (LacI) was used. LacI is a paradigmatic DNA looping transcription factor which in *E. coli*, may bind cooperatively to two of three operators inducing a DNA loop to efficiently repress the expression of three genes involved in the metabolism of lactose.^{8,9} LacI can bind to a high affinity site adjacent to the promoter (O1), a ~four-fold lower affinity, secondary site ~400 bp downstream (O2), and an ~67-fold lower affinity, tertiary site ~90 bp upstream (O3).^{10–12} A strong, symmetric operator, Os, which LacI binds with five-fold greater affinity than O1, has also been engineered.¹³ The auxiliary sites are thought to serve as reservoirs to elevate the concentration of LacI in proximity to the primary, promoter-blocking site by forming loops to deliver LacI to the primary site.¹⁴ In addition, LacI tetramers exhibit higher affinity for operators in looped as compared to unlooped DNA.¹⁵ LacI bound to an operator can block transcription initiation with up to 99.5% efficiency *in vivo*^{16,17} that depends on the promoter firing rate and whether multiple RNA polymerases act cooperatively.¹⁸ Lac repressor can also obstruct eukaryotic RNA polymerase II¹⁹ to a greater or lesser degree depending on accessory factors.²⁰

The extent to which a DNA loop accentuates the repression of transcription initiation at the lac operon has been amply characterized; however, its strength as a roadblock to an advancing transcription elongation complex has never been characterized. Therefore, in this study, the progress of RNA polymerase through LacI obstacles on torsionally relaxed, looped or unlooped DNA templates was monitored using scanning force microscopy (SFM) and magnetic tweezers (MT). As expected based on reports in the literature,¹⁴ RNA polymerase more easily surpassed LacI obstacles on lower versus higher affinity operators in unlooped DNA molecule. Surprisingly, this difference was abrogated in looped DNA molecules where LacI became a strong roadblock independently of the affinity of the operator. This is remarkable in that a LacI bound to a lower affinity, O2 operator in a looped DNA molecule blocks RNA polymerase as effectively as one bound

to an approximately 20-fold higher affinity, Os operator. Furthermore, the open and closed LacI conformations were equally good roadblocks in looped DNA templates. The data indicate that an obstacle with looped topology more effectively interferes with transcription.

Results

Measuring the probability of transcriptional progress using scanning force microscopy

Sample preparation. Scanning force microscopy was used to accurately correlate the disposition of RNA polymerase and LacI obstacles with the looped or unlooped configuration of the DNA molecule. Bound LacI is a roadblock for transcription, and reports have shown that its strength depends on the binding affinity for the operator.^{16–18} DNA molecules contained two operators for LacI separated by 400 bp, so that a lac repressor could mediate looping with negligible strain in the intervening DNA segment [Fig. 1(A)]. These molecules included either the high affinity Os or the 20-fold lower affinity O2 operator 271 bp from the transcription start site (TSS). In both constructs an O1 operator was included 669 bp from the TSS. Transcription was activated using either template with or without LacI by adding 100 μ M NTPs and incubating for 60 s. EDTA was added to interrupt transcription without dissociating RNA polymerase from the template.²¹ The sample was immediately deposited on poly-L-ornithine-coated mica, incubated 1–2 min, rinsed, and dried for imaging.

LacI has two conformations. Slow scans (5 μ m/s) over large (5 \times 5 μ m) areas produced images of hundreds of DNA molecules with and without bound RNA polymerase and/or lac repressor. Most had a bound streptavidin, which was used to mark the biotinylated downstream end of the DNA template. About 50% of the DNA molecules displayed a large, bound RNA polymerase and a high percentage of these also displayed smaller LacI particles. Different topologies were observed with both parallel and anti-parallel orientations of the DNA segments and examples of many of the conformations described previously (Supporting Information Fig. S1).²²

The LacI particles could be catalogued as either in the closed or open conformations^{22,23} that were especially clear in DNA molecules with LacI-mediated loops [Fig. 1(B)]. Each of two lobes of the tetrameric lac repressor attaches to separate DNA segments to cross link them and secure a loop. Surprisingly, there is considerable conformational flexibility in a LacI-mediated loop that allows as much as 14 nm separation between the bound DNA segments. This is likely to be important especially for

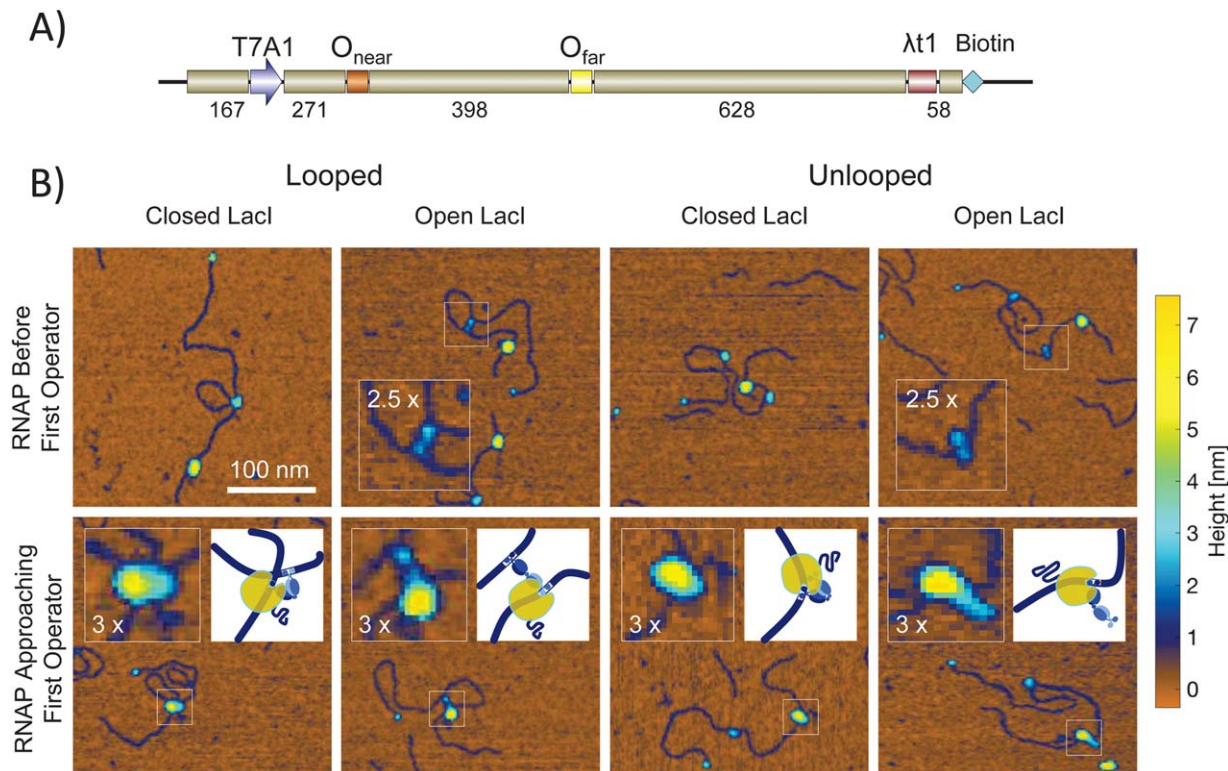


Figure 1. Nanographs of RNA polymerases trapped by EDTA quenching during elongation along DNA with and without LacI-mediated loops. (A) Schematic representation of the DNA templates used in scanning force microscopy assays. All templates contained a T7A1 promoter close to the upstream end, a stall site at position +22, a “far” O1 operator, the lambda t1 terminator ($\lambda t1$) and a biotin label at the downstream end. The two DNA templates used for SFM measurements of transcription differed in the “near” operator positioned 253 bp downstream from the promoter; one template contained the O_s operator while the other contained the O₂ operator. The terminator was the very last feature of the sequence and was biotin labeled. Streptavidin was coupled to the biotin label to facilitate identifying the “downstream” end of the molecule in SFM nanographs. (B) The upper row is a selection of molecules along which RNA polymerases (large yellow particle) had not progressed very far from the transcription start site near the end of the DNA without a streptavidin particle (blue). Closed and open conformations of the LacI tetramers are visible for either looped (left) or unlooped (right) columns. The closed conformations are shown as blue particles that are slightly larger than the streptavidin. In the open conformation, two lobes are visible especially on looped DNA. These lobes correspond to individual dimers with DNA binding head groups. The TECs shown in the lower row had progressed further and small coils of RNA emanate from them (see inset schematics for the regions of interest). These TECs have collided with LacI particles. The LacI particles correspond to blue protuberances on the periphery of the larger yellow RNA polymerase particle. The RNA polymerases themselves appear to shift to the side opposite LacI especially for open LacI conformations.

LacI to mediate loops in short and therefore stiff DNA segments such as the 93 bp loop between O₃ and O₁ in *E. coli*. It could also be important in the mechanism by which a transcription elongation complex (TEC) bypasses a LacI obstacle.

Speed of elongation. Aliquots were imaged to provide snapshots of the transcriptional progress made by RNA polymerase after 60 s of elongation with or without LacI obstacles. In the absence of LacI, transcription elongation complexes were found at various positions along the template (Fig. 2, left column; Supporting Information Fig. S2, top-left). The schematic diagram above the column indicates five segments with which RNA polymerase positions were classified (see next section). The progress of the RNA polymerase is clearly due to transcription, because the

nascent RNA grows as TECs are observed further along the template (Fig. 2 left column).

To calculate the average rate of transcription, a frequency distribution of the actual measured locations was plotted [Fig. 3(A), RNAP_{no LacI}]. This plot shows the surviving fraction of TECs as a function of the distance along the template. Some TECs remain stuck at the promoter, but almost 50% transcribe far enough to reach the “near” operator which is unoccupied in this case. The surviving TECs progress along the DNA contour until they become randomly stopped or halted by the addition of EDTA (after 60 s). This distribution of observed positions was fitted with a Gaussian to describe the number of TECs stuck at promoters (inactive) and a decaying exponential function to describe the active, elongating population (Supporting Information Fig. S3). The average progress determined from this

exponential function was 660 bp which, when divided by the incubation time, 60 s, produced an estimated average rate of elongation of 10.3 bp/s. This estimate agrees with previously reported *in vitro* rates at comparable NTP concentrations.²⁴⁻²⁶

LacI obstacles impede TECs. When LacI was added to the transcription assay, it formed roadblocks to transcription either bound to an operator along unlooped DNA, or bridging two operators to secure a loop. Additional series of nano-topographs

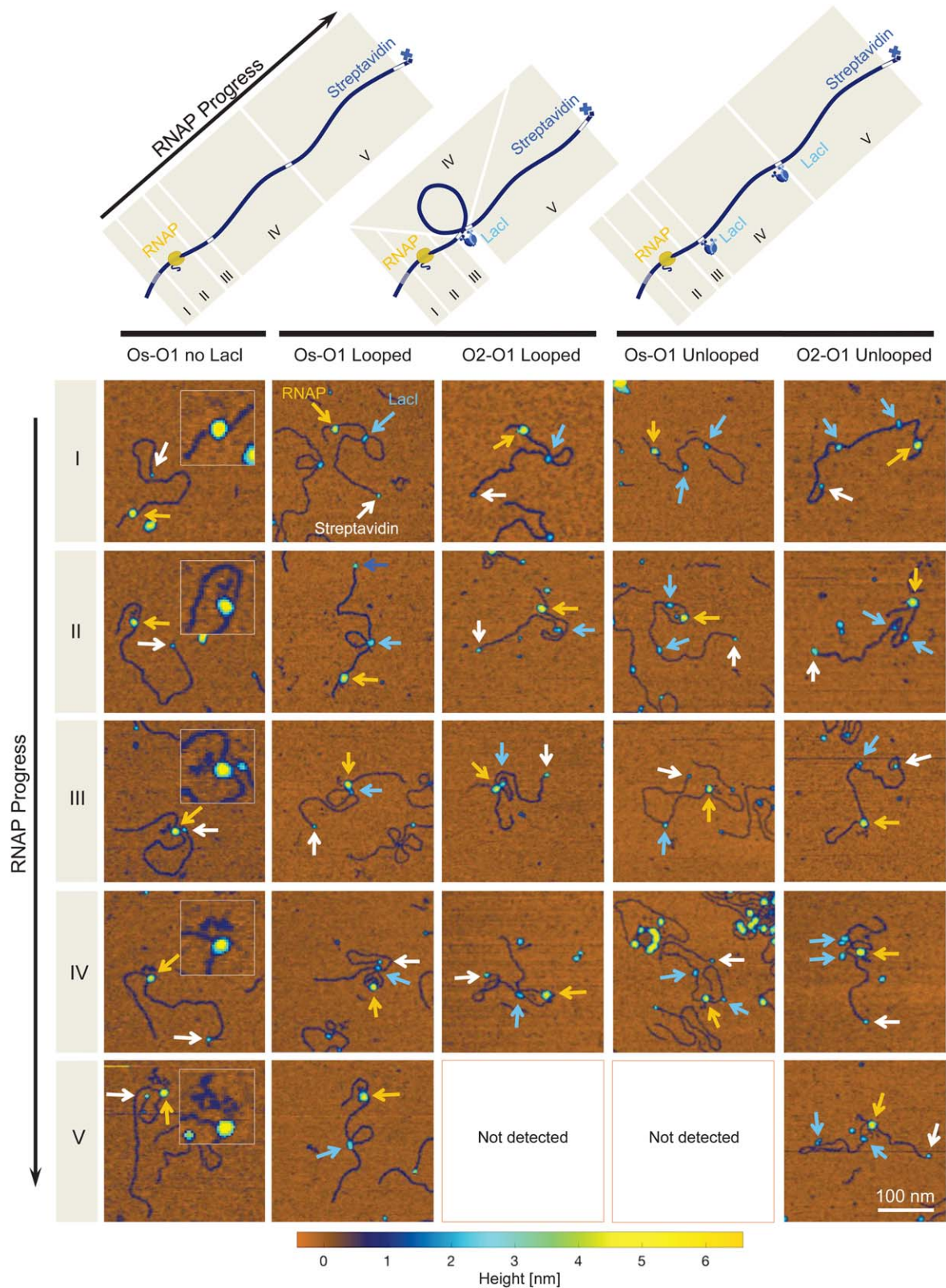


Figure 2.

in Figure 2 show RNA polymerase at different stages of elongation along looped (columns 2 and 3) or unlooped (columns 4 and 5) templates. The rows of images are ordered according to the segments depicted in schematic diagrams above each column. RNA polymerases remaining at the T7A1 promoter are pictured in the first row (I), RNA polymerases that had not yet reached the near operator are in the second row (II), RNA polymerases in close proximity to the near operator follow in the next row (III), RNA polymerases between the two operators make up the fourth row (IV), and finally RNA polymerases that surpassed even the far operator are depicted in the bottom row (V).

The graphs in Figure 3 show the surviving fraction of TECs observed as a function of distance along the templates. These two graphs summarize the probability of progress observed for TECs encountering LacI obstacles on DNA templates with either Os or O2 in the “near” operator position, 271 bp from the promoter. Both templates have an O1 operator 669 bp from the promoter. In the absence of nucleotides, RNA polymerase was found only at the promoter in DNA complexes [Fig. 3(B), RNAP_{no NTP}]. There are no surviving members of the ensemble beyond about 200 bp. The high specificity of promoter recognition displayed by RNA polymerase as well as the ability to follow elongation by monitoring the position along the DNA and the size of the nascent RNA, confirmed that elongation and roadblock effects could be studied by single molecule techniques.

Naïvely, one would expect that the ability of LacI to form a barrier to transcription depends on the affinity for the operator to which it is bound. Indeed, it is well known that LacI bound to the high affinity Os operator potentially interferes with transcriptional elongation.^{16–18} TEC observations on unlooped DNA further illustrate this point. For that case, there is a significant difference in the fraction of TECs that surpass the low-affinity O2 operator compared with the fraction that pass the high-affinity Os operator [Fig. 3(A)]. LacI bound to an O2 operator only has a slight, if not negligible, effect on halting TEC progress; of the 96 measured TECs

roughly 50% were found after the near (O2) operator (Supporting Information Fig. S2). In contrast, LacI bound to an Os operator blocks most of the TECs; only 10% surpass the obstacle.

Loops enhance interference with transcription.

Contrary to the effect on LacI obstacles along unlooped DNA, operator affinity did not modulate obstruction in looped DNA. At 7.5 nM concentration, LacI begins to saturate the high affinity operators on a DNA template. Indeed LacI binding to operators was above 90% for the Os-400-O1 template and dropped about 20% with transcription. High occupancy of both operators blocks looping and reduces the percentage of looped molecules that can be achieved at lower concentrations.²⁷ In SFM images, looped molecules constituted respectively 50 or 34% of the observations with or without transcriptional activity on the Os-400-O1 template (Supporting Information Figure S4). As expected, the fraction of LacI binding was lower for the O2-400-O1 template, as was the fraction of looped molecules, 14 or 12% with and without transcription. It is important to note for the analysis that follows, that the number of looped molecules did not decrease with transcription (+NTP).

Analysis of nano-topographs like those in Figure 2 revealed that LacI-mediated loops blocked elongation with almost 100% efficiency [Fig. 3(B)]. Whether the operator at the near position was the highest affinity Os or the 20-fold lower affinity O2, LacI secured loops blocked TECs almost completely. Only a few of the TECs that reached the near LacI obstacle surpassed it even on an O2 operator. There was a difference in the occupancy of LacI at Os and O1 binding sites between the Os-400-O1 samples prepared with and without added NTPs. However, this did not change the ability of LacI bound at Os to effectively block RNA polymerase either in the looped or unlooped configuration. Furthermore, while the occupancy of O2 sites did not change when NTP was added, LacI bound at O2 was a much more effective barrier when it secured a loop.

Figure 2. Nanographs of RNAP elongation along DNA with and without LacI-mediated loops. (Top) Schematic representations of transcription elongation complexes (TECs). Columns correspond to different DNA topologies and LacI occupancy. The first column corresponds to transcription elongation without LacI in the reaction buffer. The second and third column correspond to DNA found in a looped topology, with LacI at each of the two operators; the fourth and fifth columns correspond to unlooped DNA with both operators occupied. Transcription elongation progress is categorized in five zones (roman numerals I–V). Numerals in the schematic correspond to each row of the nanograph array. Each image in the array is representative of its corresponding category (columns) and elongation progress (rows). Image colors indicate height, according to the color scale below. RNAP, LacI and streptavidin particles are indicated by yellow, light blue, and white arrows respectively. (Row I) AFM images of RNAP bound at the T7A1 promoter. (Row II) Images in which TECs have not yet reached the near operator. (Row III) Images in which TECs contact LacI at the near operator. (Row IV) Images in which TECs were found between the two operators. (Row V) Images in which TECs were beyond the far operator. As indicated in the figure, images for RNAP in zone V were not detected for looped O2-O1 DNA and unlooped Os-O1 DNA. Note that nascent RNA associated with each TEC is visible, especially in the first column (insets), and increases in size as the RNAP progresses (I to V).

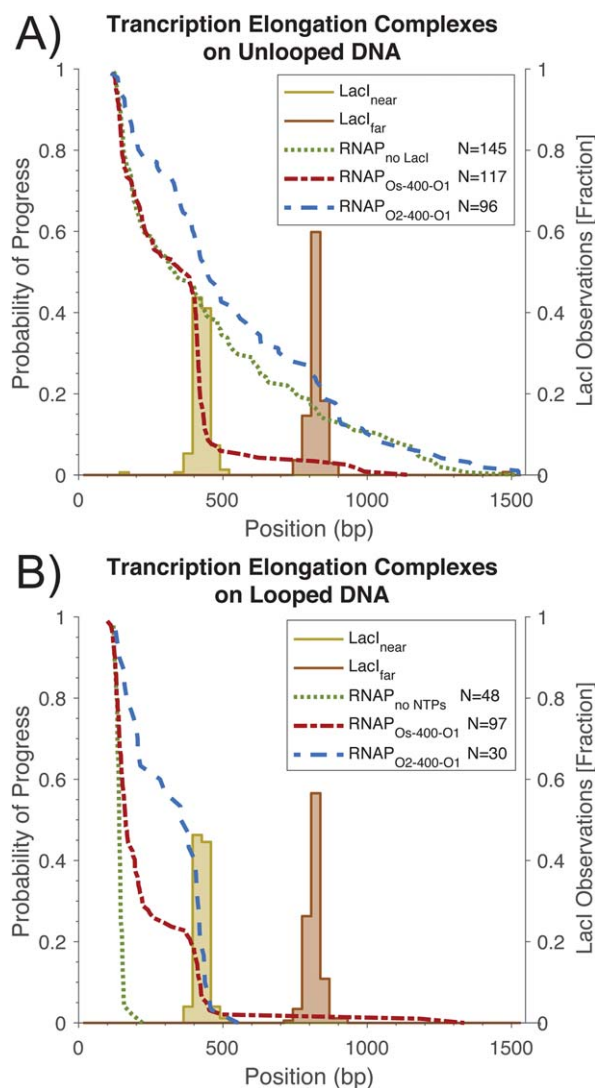


Figure 3. The probability of progress through obstacles. The positions of RNA polymerases and lac repressor molecules were measured along DNA contours in scanning force microscopy images. The probability of progress for each position was calculated as $1 - [\text{normalized cumulative histogram of RNAP position}]$. (See Supporting Information Fig. S2 for standard histograms of RNAP positions.) (A) Unlooped DNA templates. Without LacI obstacles (green dotted line), the majority of RNA polymerases began to transcribe (transcription elongation complexes, TECs) and after 60 s were distributed randomly along unlooped DNA templates. When LacI obstacles were present, a high percentage of TECs were blocked by LacI bound to the high affinity, Os operator (red, short-dashed line). In contrast, a large percentage of TECs surpassed LacI bound to the lower affinity, O2 operator (blue, long-dashed lines). (B) Looped DNA templates. Without NTPs, RNA polymerases were tightly bunched at the promoter site on DNA molecules with LacI-mediated loops (green dotted line). Almost all TECs were blocked by LacI mediating loops between O1 and the high affinity, Os operator (red, short-dashed line). Remarkably, LacI tetramers securing loops between O1 and the lower affinity, O2 operator, were equally effective obstacles (blue long-dashed line). In each graph the yellow and orange histograms indicate the distributions measured for LacI along the DNA contours.

This finding suggests that when the LacI tetramer is bivalently engaged to two operators, forming a loop, the effective affinity to both operators increases. This conclusion is further supported by the observation that activating transcription (through the addition of NTP to the reaction buffer) only slightly decreased the observed fraction of looped molecules on the O2-400-O1 DNA template and increased the looped fraction observed for the Os-400-O1 template (Supporting Information Fig. S4). It is worth noting that increased obstruction may not be solely attributable to increased affinity. In addition, the intersecting or apposed segments of DNA associated with a loop might prevent RNA polymerase from reaching a LacI obstacle. However, it is likely to be a small effect, since RNA polymerase in direct contact with the loop-LacI complex appears in nanographs such as that depicted in Row III, column 1 of Figure 2.

RNA polymerase overcomes pausing in magnetic tweezer experiments

Analysis of transcription using magnetic tweezers. To understand what happens to an RNA polymerase that encounters a LacI obstacle, the real-time progress was tracked using magnetic tweezers (Supporting Information Fig. S5). A DNA tether containing only the O1 operator was used [Fig. 4(A)], and the change in the length of the tether was monitored after a missing nucleotide was added to allow stalled RNA polymerases to resume transcription. Figure 4(B–E) shows representative traces of the average change in the extension of DNA tethers as a function of time. The DNA extension is maximal at the beginning of the experiment when TECs were stalled at position +22 for lack of CTP [Fig. 4(B–E), top dashed line at 0]. When the missing nucleotide was added, elongation resumed after random delays and was detected as a progressive decrease in tether length after turbulence subsided.

The leftmost record [Fig. 4(B)] was in the absence of LacI and transcription proceeded smoothly consuming the entire tether, so that the bead was drawn down to the glass surface. Figure 4(C–E) show transcription progress in the presence of 1 or 10 nM LacI. Pauses in tether shortening (transcription elongation) were observed at the extension corresponding to O1 (dashed line at $-0.2 \mu\text{m}$). Pauses at the roadblock were measured and are reported in Figure 5 together with the mean lifetimes of LacI-operator complexes estimated as the inverse of the measured off-rates.¹⁸ Notice that the mean pause time is similar to the average dwell time of LacI on O1 *in vitro*. Furthermore, the average pause is longer than that measured previously for TECs with no obstacles, $90 \pm 14 \text{ s}$.²⁸ Sometimes transcription ceased at the terminator [Fig. 4(C,D), dashed line at

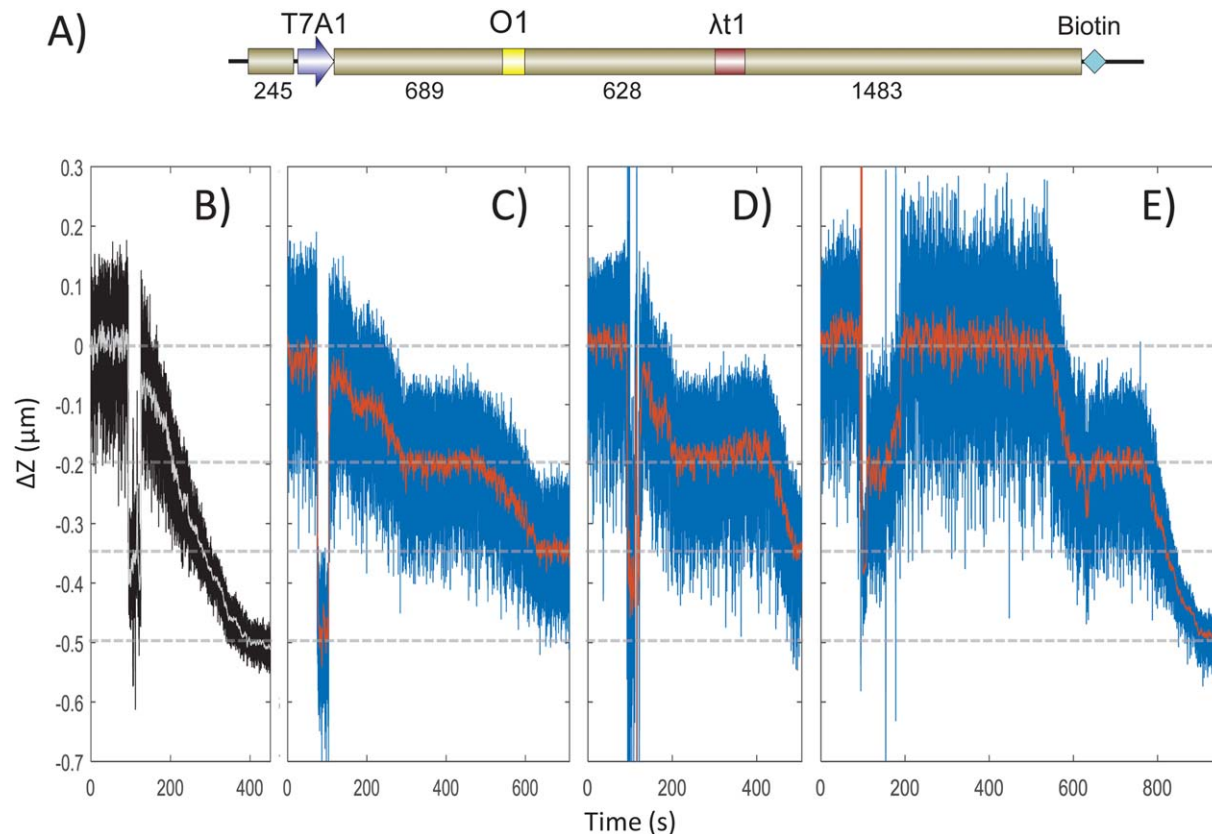


Figure 4. LacI bound to an O1 operator pauses transcription. (A) A schematic representation of the DNA template used in magnetic tweezer transcription assays. The template contained a T7A1 promoter close to the upstream end, a stall site at position +22, an O1 operator, the lambda t1 terminator ($\lambda t1$) and a biotin label at the downstream end. A streptavidin-labeled paramagnetic bead was coupled to the biotin label to for micromanipulation in the magnetic tweezer. Four examples of transcriptional elongation recorded using the magnetic tweezers are displayed. In (B) no LacI was included and transcription shortened the DNA tether progressively without interruption. When LacI was included (C–E), transcription shortened the tether by about 0.2 μm before pausing for about 200 s and then resuming. Transcription finally ceased after the tether shortened by either 0.35 μm (C and D), a distance corresponding to the location of a terminator sequence, or 0.5 μm (B and E), a distance corresponding to the end of the template.

–0.35 μm], but alternatively it continued until the bead was drawn down to the micro-chamber surface [Fig. 4(B,E), dashed line at –0.5 μm].

Discussion

Operator occupancy is likely to be very high in SFM transcription assays

It is remarkable that RNA polymerase paused for one hundred or more seconds when it encountered LacI obstacles. Although this may not be relevant in vivo where additional factors like Mfd may relieve blockages and/or dissociate elongation complexes.¹⁸ it suggests that rather than dislodging obstacles, RNA polymerase simply waits for obstacles to disappear. This is compatible with the in vivo results in which promoter firing rate and the multiplicity of paused TECs affected read through.¹⁸ Such extended pauses indicate that during a transcription interval of 60 s, LacI can resist an advancing RNA polymerase particularly when bound to a high affinity

operator like O1. For the large number of complexes analyzed using scanning force microscopy, LacI obstacles on O_s operators are likely to endure throughout the interval. Given the lower affinity of LacI for O₂, LacI obstacles on the unlooped O₂-400-O₁ templates may disappear intermittently to give RNA polymerase the opportunity to proceed, but this is probably negligible as described in the following paragraph and certainly occurs rarely in the looped conformation.

Tethering and high LacI drive operator occupancy

Assaying the position of TECs using scanning force microscopy as described requires ruling out artifacts associated with the dynamic equilibrium of LacI binding. LacI might bind to an operator after a TEC has passed through, such that in a subsequent image the TEC will appear to have surpassed a LacI obstacle. Certainly after 30 min. of incubation (see Materials and Methods), LacI has established a

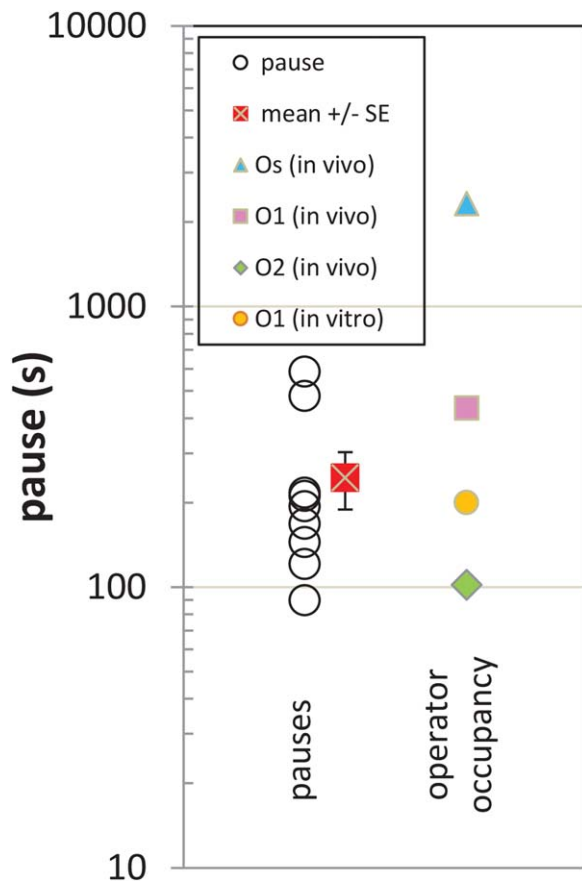


Figure 5. TEC pauses and expected operator occupancy. Sections of time series like those displayed in Figure 4 were fitted as described in Supporting Information Figure S6 to determine pause intervals at the position corresponding to the O1 operator site (○). The mean value is also plotted with standard error indicated (red x: 253). This mean is considerably shorter than expected the mean interval of occupancy of the operator *in vivo* calculated as the inverse of the reported dissociation rate of LacI from O1 (pink □: 434 s). Also shown are values for the expected mean intervals of *in vivo* occupancy of operators O2 (green ◇: 102 s) and Os (blue △: 2326 s) and *in vitro* occupancy of O1 (orange circle: 200 s).

dynamic equilibrium with operator sites along DNA molecules. However, 7.5 nM LacI fairly saturates Os operators ($K_d < 1 \times 10^{-14}$ M in similar K^+ conditions²⁹), and the estimated tether-augmented, effective concentration (J value) of LacI is expected to be in the range of 4 to 100 nM for a 400 bp loop (data not shown³⁰). Therefore, operator occupancy is expected to be very high throughout the 60 s incubation. In addition, the large association rate constant determined for similar, *in vitro* conditions, 7.9×10^9 M⁻¹ s⁻¹,²² leads one to estimate that the operator might remain unoccupied an average of 60 s. Moving at 10.3 bp/s, an RNA polymerase would traverse the near operator approximately 27 s after beginning transcription. If transcription does not begin immediately after adding NTP, then the possible time interval between the transit of an initially unoccupied operator by a TEC

followed by LacI binding to the operator becomes very short. Consequently, a negligible fraction of initially unoccupied operator sites is expected to become filled after the transit of RNA polymerase within the 60 s time window before quenching.

Does RNAP Wait for LacI to Dissociate or Does It Eject It?

Our results demonstrate that RNA polymerase halts but eventually bypasses LacI bound operator sites, especially the lower-affinity O2 operator. The propensity of RNA polymerase to bypass LacI-bound O2 is illustrated in Figure 3(A), which shows that RNA polymerase progress along the O2-O1 sequence is only marginally affected by the addition of LacI. Three factors may contribute to the ability of RNA polymerase to bypass bound O2 operators: stochastic dissociation of LacI, RNA polymerase transcribing around the obstacle, and RNA polymerase actively dislodging LacI.

It is possible that RNA polymerase dislodges LacI from its operator. RNA polymerase II effectively dislodged nucleosomes from DNA templates and was more effective at higher transcriptional velocity.² The SFM results reported here show that Os is a strong road block to transcription, even in the absence of looping [Fig. 3(A)]. The affinity of LacI for Os is about 20 times that for O2, meaning it is less likely to be dislodged by an advancing polymerase. Indeed, this is exhibited in the SFM results, in which only 10% of RNA polymerases pass a LacI bound to Os but 50% pass a LacI bound to O2 [Fig. 3(A)]. Magnetic tweezer transcription experiments utilizing DNA containing the stronger Os operator are currently in progress. Based on its dissociation rate, the occupancy lifetime of Os is expected to be roughly five times longer than O1. Consequently, changes in pause duration relative to the expected occupation time should reveal whether RNA polymerase is simply waiting for LacI to dissociate or actively dislodging the molecule.

The dissociation rates for LacI bound to DNA have been determined previously and suggest that *in vivo* LacI will dissociate after 2326, 434, or 102 s from Os, O1, and O2 respectively.¹² For *in vitro* conditions similar to those described here, the O1 dissociation rate is reported to be 0.3/min³¹; the reciprocal suggests that LacI occupies an O1 operator for an average of 200 s. In the magnetic tweezer experiments pauses at the O1 site lasted an average of 246 s. This seems to indicate that *in vitro*, without accessory factors, RNA polymerase waits for LacI to dissociate.

There is also some evidence to suggest that RNA polymerase transcribes around LacI bound to O2. In several AFM images (Fig. 1), RNA polymerase appears to be in contact with the periphery of the DNA-bound LacI. These images are qualitatively

similar to what has been reported for RNA polymerase II transcribing through nucleosomes by loop diffusion.² Based on this similarity, one might conclude that RNA polymerase bypasses LacI through a similar loop diffusion mechanism. However, it is important to note that, histone octamers exhibit lower affinity and sequence specificity for DNA and have a much larger footprint, both of which are thought to be essential for loop diffusion. By comparison, LacI is highly specific and has a smaller footprint meaning it is unlikely to be susceptible to loop diffusion. It is possible that LacI “steps” around RNA polymerase as it transcribes through the operator. In the open conformation, LacI can reach as far as 14 nm between its operator binding sites, a distance that is large enough to straddle the RNA polymerase to let it pass. This mechanism is also supported by the fact that RNA polymerase induces local bending in the DNA, which would serve to reduce the distance LacI would need to span.³²

Conclusion

Magnetic tweezers and scanning force microscopy assays showed several new features of the LacI protein. By limiting active transcription to a defined time interval, the rate of elongation was determined using scanning force microscopy. The disposition of halted RNA polymerases and LacI obstacles in nanotopographs showed the expected dependence of the probability of progress on the operator strength for unlooped templates, but even LacI on a weak operator became an efficient roadblock to transcription elongation on a looped template. Thus, while the affinity of LacI for the binding site determines the strength of the roadblock in unlooped DNA constructs, it is not as critical for looped templates. Finally, the two conformations of LacI were clearly distinguished for the first time in both unlooped and looped complexes. It remains to be seen whether they constitute roadblocks of equivalent strength, but the clear images of the open LacI conformation suggested that the protein could straddle a TEC and therefore contribute to the mechanisms that resolve TEC halting by a LacI roadblock.

Materials and Methods

DNA for scanning force microscopy

1523 bp-long DNA fragments were produced by PCR using plasmid templates, pYY_I1_400_BstEII or pZV_21_400 (Genbank format files in supplementary information), with an unlabeled forward primer and a biotin-labeled reverse primer, and purified using a QIAQuick PCR Cleanup kit (Qiagen, Germantown, MD). The fragment contained the T7A1 promoter close to the upstream end, a “near” operator 261 bp downstream, a “far” operator 669 bp downstream, the lambda t1 terminator 1298 bp downstream, and

a biotin-label at the far downstream end for tagging with streptavidin (Fig. 1).

Sample preparation for scanning force microscopy

As described in previous reports,^{33,34} shortly before deposition of the sample, a 5 μ l droplet of 0.01 μ g/ml of poly-L-ornithine (1 kDa MW, Sigma-Aldrich, St. Louis, MO) was deposited onto freshly cleaved mica and incubated for 2 min. The poly-L-ornithine-coated mica was rinsed drop-wise with 400 μ l of high-performance liquid chromatography grade water and dried with compressed air. Complexes of RNA polymerase bound at the promoter (PC) were produced by incubating 1 nM of DNA with 0.1 μ M streptavidin, 7.5 nM LacI (unless otherwise stated) and RNA polymerase holoenzyme (New England Biolabs, Ipswich, MA) diluted 200 times in transcription buffer (TXB; 20 mM Tris-glutamate (pH 8.0), 10 mM magnesium-glutamate, 50 mM potassium-glutamate, 1mM DTT) for 30 min at 37°C. To initiate transcription, the reaction mixture was spiked with 1 mM NTPs to give a final concentration of 100 μ M, and incubating at 37°C for 60 s. Elongation was terminated by spiking the mixture with 250 mM EDTA in TXB to give a final concentration of 20 mM EDTA, and incubating at 37°C for 30 s. 5 μ l of the sample solution containing DNA and proteins were deposited on the poly-L-ornithine-coated mica and incubated for 2 min. This droplet was rinsed with 400 μ l of high-performance liquid chromatography grade water and dried gently with compressed air.

Scanning force microscopy and tracing DNA contours

Images were acquired with a NanoScope MultiMode VIII AFM microscope (Bruker Nano Surfaces, Santa Barbara, CA, USA) operating in Peak Force Tapping Mode using ScanAsyst-Air cantilevers with 2 nm nominal tip radius. Areas of 5 \times 5 μ m² were scanned at a rate of 0.27 Hz with a resolution of 2560 \times 2560 pixels. After filtering the images to remove scan line offsets and tilt/bow, DNA molecules were interactively traced with the NeuronJ³⁵ plug-in of ImageJ.³⁶ For both the looped and unlooped molecules, segments between end points and proteins, or between two proteins, were measured to determine the positions of all proteins along the DNA. Figure 3 and Supporting Information Fig. S2 show the ensemble of lac repressor positions for both looped and unlooped was tightly grouped at the near and far operator sites. The observed loops were between these two positions. The position of protein along each DNA molecule was normalized by the measured DNA length of the molecule set equal to 1524 bp.

Magnetic tweezers

The real-time transcription experiments were conducted using a custom-built inverted microscope equipped with magnetic tweezers. The microscope is similar in construction to several previously described.^{37–39} Magnetic tweezers use a magnetic dipole to exert forces and torques on paramagnetic microspheres tethered to the bottom of a sample chamber by a DNA molecule (Supporting Information Fig. S5). The height of a tethered microsphere relative to the objective focal plane is measured by comparing the bright-field diffraction pattern of the bead to a previously recorded lookup table containing bead-diffraction patterns as a function of objective position. The length of the tether can be calculated by subtracting the relative height of the tethered particle from the relative height of a reference particle bound to the chamber surface (Supporting Information Fig. S5).

The microscope was assembled using a Nikon Plan 100x/1.25 Oil immersion objective (Nikon Instruments Inc. Melville, NY), P-721 Piezo Flexure Objective Scanner (PI Physik Instrumente LP Auburn, MA), an $f = 160$ mm tube lens (Thorlabs Inc. Newton, NJ), and a Basler acA2000-165um camera (IVS Imaging, Coppel, TX). Samples were illuminated using a custom LED (Luxeon Star LEDs, Quadica Developments Inc. Brantford, ON, Canada), bright-field illuminator. The magnetic dipole consisted of two $1/2 \times 1/4 \times 1/8$ inch Neodymium N52 grade magnets (K&J Magnetics Inc. Pipersville, PA), spaced 1 mm apart, attached to a steel hub, mounted on a vertical translation and rotation stage (custom design) along the bright-field beam path.

Real-time 3D particle tracking was implemented following a previously published scheme.⁴⁰ The XY-location of each particle was tracked using a radial symmetry detection algorithm.⁴¹ The combination of objective, lens, and camera yielded a pixel resolution of 72.5 nm/pixel. With moderate image noise the radial symmetry algorithm localized particles to within 5–10% of a pixel, yielding an effective lateral accuracy of around 3–7 nm. Z-positions were determined by matching the radial profile of diffraction pattern intensity (\hat{I}_r) with the intensity pattern in the lookup table ($I_r[z]$) that yielded the smallest total squared difference $\left(\text{argmin}\left[\sum_r (I_r[z] - \hat{I}_r)^2\right]\right)$. For these experiments a finite sampled lookup table ($I_r[z_k]$, with $k = 1, 2, \dots$) was used. The sub-step height was calculated by fitting the squared intensity differences to a parabola and using the vertex as the best estimate of Z. Calibration experiments revealed that this scheme yielded a depth resolution of 10–20 nm. Microscope controls and 3D tracking software were written in MATLAB (Mathworks Natick, MA) and utilize Micro-manager (www.micro-manager.org) to communicate with the hardware. Tracking routines and control

software can be found at <http://www.physics.emory.edu/faculty/finzi/research/code.shtml>.

DNA for MT

A 3025 bp DNA fragment was produced by PCR using a plasmid template, pYY_N1400_BstEII (Supplementary information F1), with an unlabeled forward primer and a biotin-labeled reverse primer, and purified using a QIAQuick PCR Cleanup kit. The template contained the T7A1 promoter close to the upstream end, an O1 operator 689 bp downstream, the lambda t1 terminator 1298 bp downstream, and a biotin at the far, downstream end for attachment to a streptavidin-coated bead [Fig. 4(A)]. The DNA template encoded only A, G, and U ribonucleotides until +22, in order to be able to stall the transcription elongation complex (TEC) by withholding CTP.

Sample preparation for magnetic tweezers

Chambers were prepared as previously reported.^{42,43} In brief, micro-chambers with an approximate volume of ~ 30 μL were prepared using a laser-cut Parafilm gasket, which was heated to seal it between two coverslips (Fisherbrand, Thermo Fisher Scientific, Waltham, MA), cleaned with laboratory soap, rinsed with water, and stored in ethanol. The inlet and outlet channels were narrow to reduce evaporation of solution.⁴⁴ The chamber was then incubated with 10 $\mu\text{g}/\text{mL}$ purified Anti-HA 11 Epitope tag antibody (16B12, monoclonal, Biolegend, San Diego, CA) in TXB (without magnesium glutamate) at 4°C overnight (≤ 16 hrs) or at room temperature for 1 hr. Then, the surface was passivated with TXB (without magnesium glutamate) supplemented with 3 mg/mL α -casein (Sigma-Aldrich, St. Louis, MO) at room temperature for 1 h.

Stalled elongation complexes (SECs) were produced by incubating 25 nM doubly-HA tagged *E. coli* RNA polymerase (Karen Adelman Laboratory, NIH), 10 nM DNA template, 50 μM GpA (initiating dinucleotide), and 10 μM ATP/UTP/GTP in TXB supplemented with 0.2 mg/mL α -casein at 37°C for 30 mins. SECs were then drawn into the chamber and incubated 30 min at room temperature to let the HA-labeled RNA polymerase bind to the anti-HA-coated surface. The far end of the DNA from the promoter was then labeled with a 1.0 μm diameter, streptavidin-coated paramagnetic bead (Dynabead MyOne Streptavidin T1, Invitrogen, Grand Island, NY) by incubating it with 20 $\mu\text{g}/\text{ml}$ for 15 min. The experimental construct in the magnetic tweezers microscope is schematically illustrated in Supporting Information Figure S5. The extension of the DNA tether was monitored after introducing 1 mM NTPs with/without LacI (10 nM or 1 nM) in TXB supplemented with 0.2 mg/mL α -casein.

Acquisition and analysis of magnetic tweezer data

Extension-versus-time data were acquired at 164 Hz using a custom-built instrument. The single biotin label at the end far from the T7A1 promoter acted as a swivel to torsionally relax the tether during transcription. Before adding NTPs, the extension of the tether was recorded for approximately 1 minute. Immediately after addition of 1 mM NTPs, turbulence lasting almost one minute produced spurious length measurements. When the turbulence subsided, many tethers returned to the previously measured extension value and shortly thereafter transcription elongation resumed and the DNA extension decreased.

A 60-point moving average of the motions of beads that were stuck to the surface was used to subtract mechanical drift introduced by vibration or thermal expansion of the microscope. A 200-point moving average of the drift-corrected time-series was applied to abate the noise in each time series. Pausing times were estimated as illustrated in Supporting Information Figure S6 by fitting sections of the time series with linear functions representing (1) transcription before pausing, (2) pausing, and (3) transcription after pausing. The duration of a pause was estimated as the distance between the intersections of lines 1 and 2 and lines 2 and 3.

Acknowledgment

We would like to thank Karen Adelman for 2HA-RNA polymerase, Kathleen Matthews for the LacI protein, and Jie Ma for useful discussion on transcription assays in the magnetic tweezers setup.

References

1. Hodges C, Bintu L, Lubkowska L, Kashlev M, Bustamante C (2009) Nucleosomal fluctuations govern the transcription dynamics of RNA polymerase II. *Science* 325:626–628.
2. Bintu L, Kopaczynska M, Hodges C, Lubkowska L, Kashlev M, Bustamante C (2011) The elongation rate of RNA polymerase determines the fate of transcribed nucleosomes. *Nat Struct Mol Biol* 18:1394–1399.
3. Bintu L, Ishibashi T, Dangkulwanich M, Wu YY, Lubkowska L, Kashlev M, Bustamante C (2012) Nucleosomal elements that control the topography of the barrier to transcription. *Cell* 151:738–749.
4. Jin J, Bai L, Johnson DS, Fulbright RM, Kireeva ML, Kashlev M, Wang MD (2010) Synergistic action of RNA polymerases in overcoming the nucleosomal barrier. *Nat Struct Mol Biol* 17:745–752.
5. Zhang T, Cooper S, Brockdorff N (2015) The interplay of histone modifications – writers that read. *EMBO Rep* 16:1467–1481.
6. Long Hannah K, Prescott Sara L, Wysocka J (2016) Ever-changing landscapes: transcriptional enhancers in development and evolution. *Cell* 167:1170–1187.
7. Mendes MA, Guerra RF, Berns MC, Manzo C, Masiero S, Finzi L, Kater MM, Colombo L (2013) MADS domain transcription factors mediate short-range DNA looping

that is essential for target gene expression in Arabidopsis. *Plant Cell* 25:2560–2572.

8. Matthews KS (1992) DNA looping. *Microbiol Rev* 56: 123–136.
9. Wilson CJ, Zhan H, Swint-Kruse L, Matthews KS (2007) The lactose repressor system: paradigms for regulation, allosteric behavior and protein folding. *Cell Mol Life Sci* 64:3–16.
10. Hsieh WT, Whitson PA, Matthews KS, Wells RD (1987) Influence of sequence and distance between two operators on interaction with the lac repressor. *J Biol Chem* 262:14583–14591.
11. Pfahl M, Gulde V, Bourgeois S (1979) “Second” and “third operator” of the lac operon: an investigation of their role in the regulatory mechanism. *J Mol Biol* 127: 339–344.
12. Garcia HG, Phillips R (2011) Quantitative dissection of the simple repression input-output function. *Proc Natl Acad Sci USA* 108:12173–12178.
13. Sadler JR, Sasmor H, Betz JL (1983) A perfectly symmetric lac operator binds the lac repressor very tightly. *Proc Natl Acad Sci USA* 80:6785–6789.
14. Oehler S, Müller-Hill B (2010) High local concentration: a fundamental strategy of life. *J Mol Biol* 395: 242–253.
15. Whitson PA, Hsieh WT, Wells RD, Matthews KS (1987) Influence of supercoiling and sequence context on operator DNA-binding with lac repressor. *J Biol Chem* 262: 14592–14599.
16. Oehler S, Amouyal M, Kolkhof P, von Wilcken-Bergmann B, Muller-Hill B (1994) Quality and position of the three lac operators of *E. coli* define efficiency of repression. *EMBO J* 13:3348–3355.
17. Deuschle U, Gentz R, Bujard H (1986) lac repressor blocks transcribing RNA polymerase and terminates transcription. *Proc Natl Acad Sci USA* 83:4134–4137.
18. Hao N, Krishna S, Ahlgren-Berg A, Cutts EE, Shearwin KE, Dodd IB (2014) Road rules for traffic on DNA-systematic analysis of transcriptional roadblocking in vivo. *Nucleic Acids Res* 42:8861–8872.
19. Deuschle U, Hipskind RA, Bujard H (1990) RNA polymerase II transcription blocked by *Escherichia coli* lac repressor. *Science* 248:480–483.
20. Reines D, Mote J Jr (1993) Elongation factor SII-dependent transcription by RNA polymerase II through a sequence-specific DNA-binding protein. *Proc Natl Acad Sci USA* 90:1917–1921.
21. Arndt KM, Chamberlin MJ (1990) RNA chain elongation by *Escherichia coli* RNA polymerase - factors affecting the stability of elongating ternary complexes. *J Mol Biol* 213:79–108.
22. Wong OK, Guthold M, Erie DA, Gelles J (2008) Interconvertible lac repressor-DNA loops revealed by single-molecule experiments. *PLoS Biol* 6:e232.
23. Rutkauskas D, Zhan H, Matthews KS, Pavone FS, Vanzi F (2009) Tetramer opening in LacI-mediated DNA looping. *Proc Natl Acad Sci USA* 106:16627–16632.
24. Davenport RJ, Wuite GJ, Landick R, Bustamante C (2000) Single-molecule study of transcriptional pausing and arrest by *E. coli* RNA polymerase. *Science* 287: 2497–2500.
25. Neuman KC, Abbondanzieri EA, Landick R, Gelles J, Block SM (2003) Ubiquitous transcriptional pausing is independent of RNA polymerase backtracking. *Cell* 115:437–447.
26. Schafer DA, Gelles J, Sheetz MP, Landick R (1991) Transcription by single molecules of RNA polymerase observed by light microscopy. *Nature* 352:444–448.

27. Johnson S, Lindén M, Phillips R (2012) Sequence dependence of transcription factor-mediated DNA looping. *Nucleic Acids Res* 40:7728–7738.
28. Forde NR, Izhaky D, Woodcock GR, Wuite GJ, Bustamante C (2002) Using mechanical force to probe the mechanism of pausing and arrest during continuous elongation by *Escherichia coli* RNA polymerase. *Proc Natl Acad Sci USA* 99:11682–11687.
29. Levandoski MM, Tsodikov OV, Frank DE, Melcher SE, Saecker RM, Record Jr TM (1996) Cooperative and anticooperative effects in binding of the first and second plasmid *Osym* Operators to a LacI tetramer: evidence for contributions of non-operator DNA binding by wrapping and looping. *J Mol Biol* 260:697–717.
30. Priest DG, Cui L, Kumar S, Dunlap DD, Dodd IB, Shearwin KE (2014) Quantitation of the DNA tethering effect in long-range DNA looping in vivo and in vitro using the Lac and λ repressors. *Proc Natl Acad Sci USA* 111:349–354.
31. Johnson S, van de Meent JW, Phillips R, Wiggins CH, Linden M (2014) Multiple LacI-mediated loops revealed by Bayesian statistics and tethered particle motion. *Nucleic Acids Res* 42:10265–10277.
32. Ruff E, Record M, Artsimovitch I (2015) Initial events in bacterial transcription initiation. *Biomolecules* 5:1035.
33. Wang H, Finzi L, Lewis DE, Dunlap D (2009) AFM studies of lambda repressor oligomers securing DNA loops. *Curr Pharm Biotechnol* 10:494–501.
34. Wang H, Dodd IB, Dunlap DD, Shearwin KE, Finzi L (2013) Single molecule analysis of DNA wrapping and looping by a circular 14mer wheel of the bacteriophage 186 CI repressor. *Nucleic Acids Res* 41:5746–5756.
35. Meijering E, Jacob M, Sarria JC, Steiner P, Hirling H, Unser M (2004) Design and validation of a tool for neurite tracing and analysis in fluorescence microscopy images. *Cytometry A* 58:167–176.
36. Schneider CA, Rasband WS, Eliceiri KW (2012) NIH Image to ImageJ: 25 years of image analysis. *Nat Meth* 9:671–675.
37. Riebeck N, Saleh OA (2008) Multiplexed single-molecule measurements with magnetic tweezers. *Rev Sci Instrum* 79:094301.
38. Seol Y, Neuman KC (2011) Magnetic tweezers for single-molecule manipulation. *Methods Mol Biol* 783:265–293.
39. Ding Y, Manzo C, Fulcrand G, Leng F, Dunlap D, Finzi L (2014) DNA supercoiling: a regulatory signal for the λ repressor. *Proc Natl Acad Sci USA* 111:15402–15407.
40. Gosse C, Croquette V (2002) Magnetic tweezers: micro-manipulation and force measurement at the molecular level. *Biophys J* 82:3314–3329.
41. Parthasarathy R (2012) Rapid, accurate particle tracking by calculation of radial symmetry centers. *Nat Methods* 9:724–726.
42. Kumar S, Manzo C, Zurla C, Ucuncuoglu S, Finzi L, Dunlap D (2014) Enhanced tethered-particle motion analysis reveals viscous effects. *Biophys J* 106:399–409.
43. Priest DG, Kumar S, Yan Y, Dunlap DD, Dodd IB, Shearwin KE (2014) Quantitation of interactions between two DNA loops demonstrates loop domain insulation in *E. coli* cells. *Proc Natl Acad Sci USA* 111: E4449–44E4457.
44. Kovari DT, Yan Y, Dunlap D, Finzi L (2017) Tethered particle motion: an easy technique for probing DNA topology and transcription factor interactions. *Methods Mol Biol* in press.